Tellus (1996), 48A, 324–341
Printed in Belgium – all rights reserved

TELLUS
ISSN 0280–6495

A numerical study of the water exchange through the Danish Straits

By E. SAYIN and W. KRAUSS*, *Institut für Meereskunde an der Universität Kiel, 24105 Kiel, Germany*

(Manuscript received 9 January 1995; in final form 3 July 1995)

ABSTRACT

The free surface version of the GFDL model is used to study inflow and outflow through the Danish Straits, which connect the Baltic with the North Sea. Three problems are addressed: (i) the piling up of inflowing water in the Arkona basin; (ii) the transport ratios between Belt and Sound; (iii) the dominance of hydraulic or geostrophic control. Model results show that a cyclonic eddy (dome) is formed by the inflowing saline water that prevents this water from passing rapidly into the Bornholm basin. This eddy is enforced with increasing inflow due to a sea level difference between Kattegat and western Baltic. If density gradients along the straits are weak and the flow is dominantly driven by sea level differences between Kattegat and Baltic, the well-known ratio of 70% : 30% for the transports through Belt and Sound are confirmed. Strong density gradients can change this ratio considerably, especially in the outflow case, when the light water of the Baltic flows against the heavier water of the Kattegat. Under variable wind conditions, no fixed ratio is found. The flow in the Straits is geostrophically controlled; however, the strong baroclinic density field does not allow us to derive the transport simply from sea level inclination.

1. Introduction

The Danish Straits are narrow and shallow channels that connect the Baltic Sea and the Kattegat. They are of fundamental importance for the water exchange between both areas (Fig. 1).

The Kattegat is a shallow area with a mean depth of only 23 m, which is open to the North Sea. In the upper 15 m, the water is partly of Baltic origin with salinities between 15 and 30 units. Below that layer, salinity increases to 30–35 units and forms a strong contrast to the western Baltic. The Samsö Sill (26 m) separates the Kattegat from the Belts. The Belt Sea with its deep channels, the Great Belt and the Fehmarnbelt, is 13 m deep on the average. The Great Belt is only 8 km wide at its narrowest part yielding a cross section of 255000 m^2. Darss Sill (18 m) separates the Belt Sea from the Arkona Basin, where depth reaches 45 m. Salinity in the upper 30 m in the Arkona Basin is typically 8 units and increases to about 16 units near the bottom.

The second connection between the Kattegat and the Arkona Basin is the Sound. It consists of two narrow channels east of Copenhagen, the western one, Drogden, has a sill depth of 8 m and the cross-section is approximately 80000 m^2.

The third channel between Kattegat and Western Baltic is the Little Belt, having a cross section of only 16000 m^2. This strait will not be considered in this paper.

The water and salt exchange through these straits has been studied by many oceanographers in the past. A good review, both on measurements and models up to the late 70's, was given by Jacobsen (1980); the most recent modelling development may be found in Lehmann (1995). Generally, during periods of weak and moderate winds, a two-layer system of currents prevails in the Belt, with outflow from the Baltic in the upper and inflow in the deeper layer. This bi-directional flow is density-driven, by the contrast in salinity: 30–35 units in the deeper layers of the Kattegat

* Corresponding author.

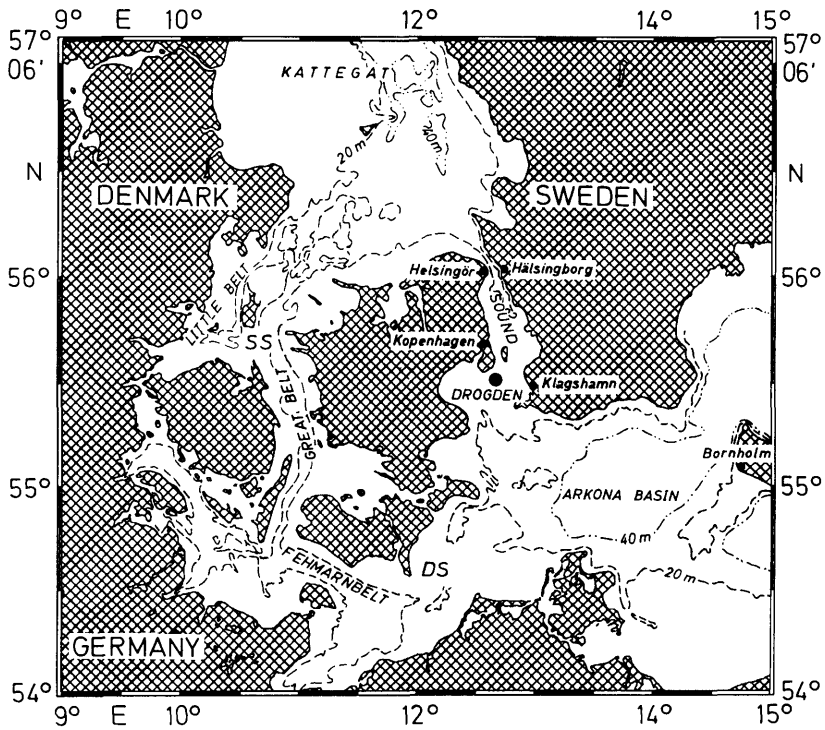

Fig. 1. The Danish Straits, Kattegat and Arkona Basin. SS = Samsö Sill. DS = Dars Sill. The Belt Sea is the area between Kattegat and Arkona basin.

and only 8 units in the upper layers of the Arkona Basin. The bi-directional flow includes the outflow from the Baltic due to the fresh water surplus.

In contrast to that, during periods of strong wind, either inflow or outflow occurs in the entire water column. Then, the main driving force is the sea level inclination between Kattegat and Arkona Basin. The flow in the shallow Sound is unidirectional at almost any time. It is general believed that about 70% of the flow occur through the Belt. This figure goes back to Jacobsen (1925) who derived transports through the straits using surface current measurements from light-ships for the period 1910–1916. Jacobsen (1980) gives the ratio 7 : 3 : 1 for Great Belt, Sound and Little Belt. However, there has been no possibility yet to verify this ratio under different wind conditions. The main problem is that the water exchange is highly variable, the ratio of the standard deviation to the long term mean being of the order of 10 (Jacobsen, 1980). Furthermore, the currents can be highly sheared, both with respect to horizontal and vertical direction. When sea level forcing dominates, stratification gives no indication of the flow direction.

Bi-directional flow is often observed in the summer months or during calm wind situations. During most of the year, bi-directional flow occurs in the Fehmarnbelt. This is observed in 50% of all cases in summer and 29% in winter (Wyrtki, 1954). In the Great Belt the corresponding numbers are 95% in summer and 65% in winter (Farmer and Møller, 1990).

A great number of numerical models of the Baltic appeared in the literature. Most of them are simplified by specific assumptions, for example the box models by Walin (1977), Svansson (1980), Rahm (1985) and Omstedt (1990), or models based on hydraulic control by Welander (1974) and Stigebrandt (1983). Besides these, a very extensive literature exists about control models and their application to the dynamics in straits.

Recent hydraulic model studies on two-layer exchange through the Strait of Gibraltar have been done by Bormans and Garrett (1989), Dalziel (1990), Garrett et al. (1990) and Bryden and Kinder (1991). Hogg (1983, 1985) developed a multi-layer hydraulic model and applied it to the Vema Channel and to the circulation in the Alboran Sea.

In the Belt, a salinity front separates the two water masses. During periods of strong easterly winds this front is shifted towards the Kattegat and reaches from the surface down to the bottom. Strong westerly winds move the front towards Darss Sill, where it also cuts both the surface and the bottom. Only during calm periods the boundary between the two water masses is mainly horizontal, reaching the surface in the northern Belt (Mälkki and Tamsalu, 1985).

In view of the complex topography, the complicated coast lines, the strong density gradients, and the variable wind conditions it is unlikely that one simple control mechanism can describe inflow and outflow properly. 3-dimensional models of the full hydrodynamic equations with high vertical and horizontal resolution are ultimately required for an adequate description of the situation. Such a model is presently used at the IfM Kiel (Lehmann, 1992, 1995), however, its horizontal resolution is 5 km only. Thus, it does not resolve the narrow straits with the required accuracy in order to study details of the strait dynamics.

In the present article, we use this same free surface version of the GFDL model (Killworth et al., 1989) for a limited area, extending from the northern Kattegat towards Bornholm. The model is run with high vertical and horizontal resolution (12 layers, $\Delta x = 2.5$ km). The basic equations of the model are the nonlinear equations of motion, continuity equation, nonlinear equations for the conservation of heat and salt, hydrostatic equation, and the equation of state.

We want to study the flow through the Danish Straits due to sea level and density differences between the Baltic and the Kattegat. The sea level difference can be maintained as follows (Fig. 2b). The real model domain is the range $L_1 < y < L_2$. Two "restoring zones", $0 < y < L_1$ and $L_2 < y < L$, are added at both ends. Within these zones equal but opposite mass transports are described through the sea surface in the continuity equation. The resulting steady sea level difference between the restoring zones depends on the friction in the

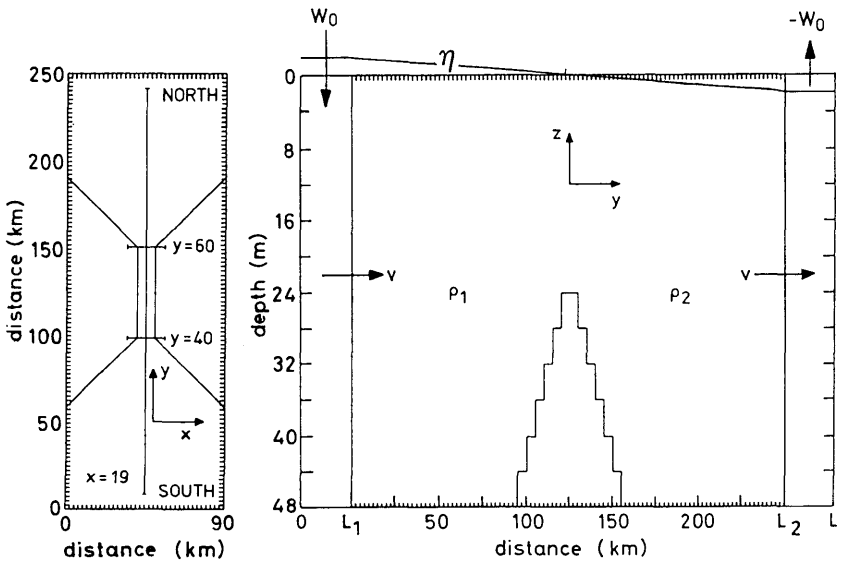

Fig. 2. Top (to the left) and side view (to the right) of the model basin. Horizontal and vertical resolution is 2.5 km and 4 m, respectively. The basin is 250 km long, 90 km wide and 48 m deep. Central line (in the left figure) shows the position of the vertical section along the channel, $\rho_2 > \rho_1$. Within the restoring zones (O, L_1) and (L_2, L) constant sea level is produced by mass supply (extraction) through the sea surface.

model. The flow through the surface per unit width, $w_0 L_1$, equals the barotropic flow uH trough L_1, L_2, H being the depth. Thus, $w = \pm w_0$ for $y < L_1$ and $y > L_2$, respectively, is the driving mechanism. At $y = 0$ and $y = L$, the model is closed.

In the simple one-dimensional linear non-rotating case, the stationary solution consists of (nearly) constant sea levels in the restoring zones and a linear inclination in the real domain. Consequently, u increases linearly from the walls and remains constant in the interior. The solution corresponds to that obtained by prescribing the barotropic flow at L_1 and L_2. For the real Baltic, the results obtained by this method have been compared to the results of an open boundary model. The barotropic flow in the interior reaches a steady level after about 3 days. The computations have been extended over 12 days for the following reasons.

(i) To damp progressive inertia-gravity waves and artificial seiches produced in the basins during the initial phase. They decay within a few periods and disappear after 3–4 days. The purely density driven case occurs in the Danish Straits only over one to two weeks.

(ii) To avoid artificial boundary effects in the baroclinic field. As outlined above, initially a frontal zone in the central area of the basin separates Baltic water from Kattegat water. This front is advected by the barotropic current (and the baroclinic dynamics) towards the restoring zone, where unrealistic dynamics are prescribed. The experiments show that a period of 12 days is long enough to describe the dynamics in the Danish Straits and in the adjacent western Arkona basin without being influenced by the restoring zones.

The objective of this study is to clarify 3 aspects of the flow in the Belt Sea and in the Arkona basin.

(i) Under which conditions does a large eddy develop at the downstream exit of the strait that prevents the water from flowing rapidly through the adjacent basin? In the Arkona basin it is known from observations that the inflowing heavy water remains there as a pool over extended periods.

(ii) Can the ratio of 70% : 30% between the transports through Great Belt and Sound be used both for inflow and outflow conditions?

(iii) Does hydraulic control, which has been assumed for many straits, play any rôle in the Danish Straits?

The paper is structured as follows. In Section 2, we study the formation of a dome-like eddy at the exit of a strait under idealized conditions: a sill in a channel, which connects two basins (two-basin experiment). Section 3 describes the mass transport through Belt and Sound, in Section 4, we test control relations for straits and in Section 5, we draw some final conclusions.

2. The two-basin experiment

We consider the basins shown in Fig. 2, which are connected by a strait. Initially, a barrier separates two fluids of different density, ρ_1 and ρ_2. The density difference is based on a salinity difference. Temperature is kept constant. The strait has a width of 10 km and a length of 50 km. Sill depth is 28 m and basin depth 48 m. We are interested in the development of currents and stratification with time. A simple geometry has been chosen in order to elucidate the main effects that may be modified and hidden under the real geometry of the Danish Straits.

Two cases will be discussed in detail: the purely density driven circulation and the forced case in which a sea level gradient is imposed additionally.

2.1. The density driven case

In Fig. 3, we depict density and current fields for the upper and lower levels (layers 1 and 13, respectively). Initially two water masses, ρ_1 and ρ_2, with a density difference of $\Delta\sigma_T = 9.5$ units are separated over the barrier. This difference corresponds to a salinity difference of 12 units at 15°C. The distributions shown in Fig. 3 have developed after 12 days. During the initial phase, Kelvin waves emerge at the front in the upper layers and propagate counterclockwise around the northern basin. The light water from the southern basin flows along the eastern coast of the northern basin with a sharp density front towards the surrounding waters. The heavier water of the northern basin penetrates into the southern basin in the deeper layer and fills this basin by a counter-

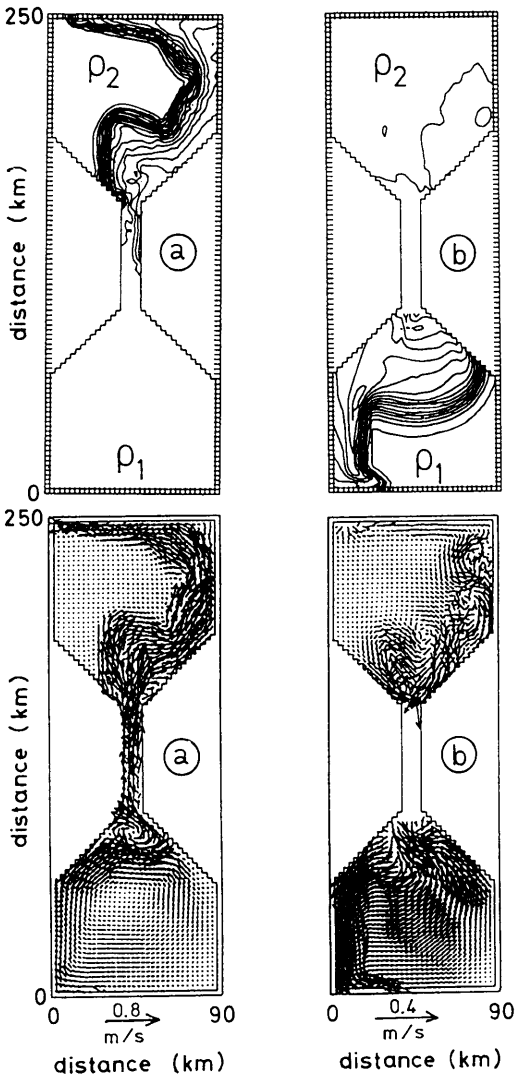

Fig. 3. Density and current fields in layers 1 and 13 (a, b) for the density driven case. Maximum velocities are 0.78 m/s for layer 1, 0.30 m/s for layer 13.

clockwise flow. At the southern entrance of the channel a cyclonic eddy is formed which reaches almost from top to bottom. In the centre of the channel, where initially the front separated the two water masses over the barrier, the Coriolis force deflects the fresh water and hence the current of the upper layers to the eastern wall.

In the northern part of the channel, the dense water occupies the entire water column below 10 m. Intensive outflow of light water occurs on the right-hand side of the channel in the upper 2 layers towards north (Fig. 3a). In the southern part of the channel, the dense water, after crossing the sill, is geostrophically inclined towards the western wall and the fresh water of the southern basin occupies most of the water column. Thus we find bottom intensification of the dense flow and surface intensification of the shallow flow after crossing the sill.

The cyclonic eddy (Fig. 3) is formed at the southern end of the channel by the heavy water after crossing the sill. This eddy is best seen in a meridional section (Fig. 4). The overflow of heavy water over the sill occurs in a shallow layer. The water accumulates at the lower rim of the sill and the density contrast to the surrounding waters induces a cyclonic circulation around this dome.

The energy transfer and the interactions between the internal and the external mode are depicted in Fig. 5 for the end of the model run. This figure shows values of the energy transfer terms and of the kinetic energy of internal (K_i) and external modes (K_e). Internal kinetic energy amounts to 57.5% of the total kinetic energy, the remaining 42.5% are external kinetic energy. Further notations are: NL is the sum of the nonlinear transfer terms, LF lateral friction, BF bottom friction, PF

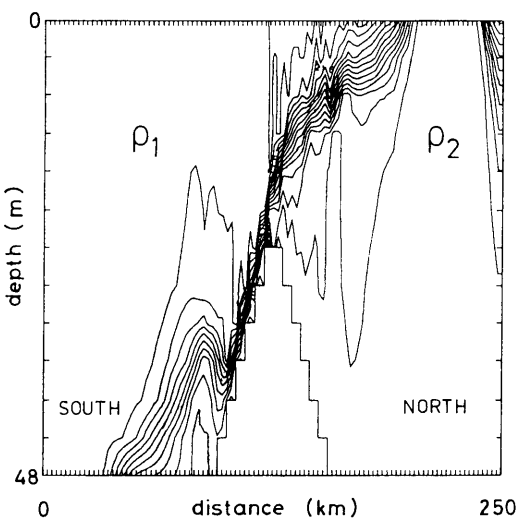

Fig. 4. Density field along the channel in the density-driven case. Location of the section is given in Fig. 2 (left).

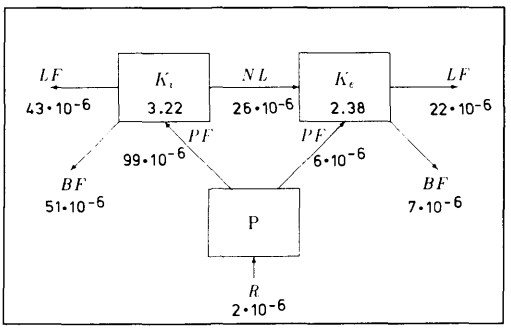

Fig. 5. Energy cycle for the density driven case. Energy transfers are shown by arrows in J m^{-3} s^{-1}.

pressure forces and R residual terms, mainly diffusion and convection. More information about these terms are found in Böning (1989).

Due to convection and diffusion the potential energy changes. This is seen, e.g., in the dome in Fig. 4. The spreading of the isopycnals in this eddy is due to convection.

The dominant transfer from potential to kinetic energy via the pressure forces feeds the internal modes. The transfer to external kinetic energy (K_e) by pressure terms is small compared to this amount. K_e gains most energy from K_i through the nonlinear terms. Both, internal and external kinetic energy have losses due to lateral and bottom friction.

In the free surface version of the Bryan-Cox-Semtner model, the depth integrated flow is not precisely the barotropic mode. Therefore, some energy leakage between barotropic and baroclinic modes is possible.

2.2. *The forced case*

In the forced case, we prescribe, additionally to the density gradient, different sea levels in the northern and southern restoring zones according to the mechanism outlined in the introduction. The level η remains fixed within a strip of 10 grid points near the northern and southern boundaries of the basins and changes initially linear within the basin. To obtain inflow into the southern basin,

$$\eta = \begin{cases} -\eta_0 & \text{for } y < 10, \quad t \geqslant 0, \\ \eta_0 & \text{for } y > 90, \quad t \geqslant 0, \end{cases}$$

has been chosen, where $\eta_0 = 0.05$ m in the present case.

Density and current distributions after 12 days are depicted in Fig. 6, showing outflow from the northern basin at all levels. Thus, the barotropic flow dominates the current field. The cyclonic eddy near the southern end of the channel becomes stronger in the forced case. A further important difference is that this cyclonic eddy is advected away from the channel, more into the centre of the southern basin.

Instead of a bi-directional flow, an unidirectional one is established in the entire channel.

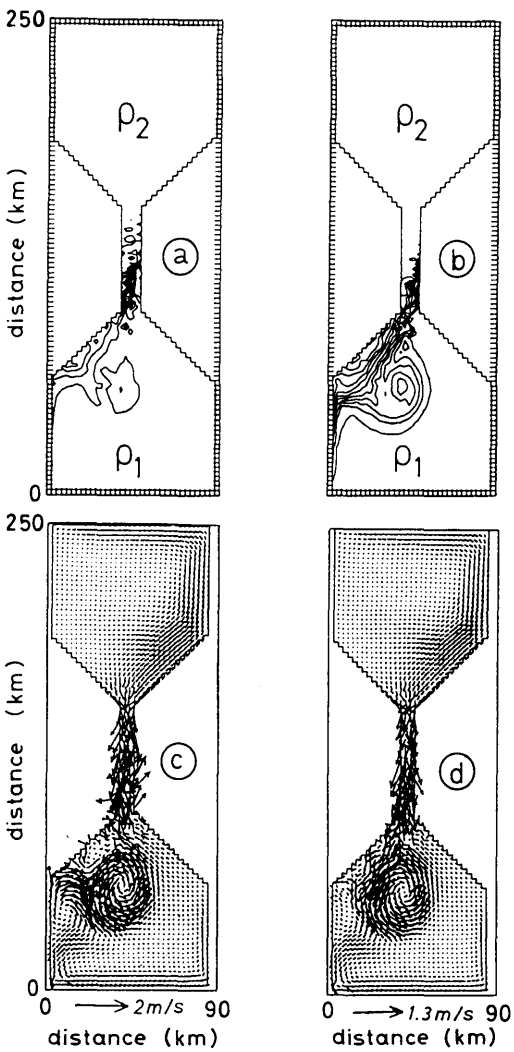

Fig. 6. Density and current fields in layers 1 and 5 (a–d). Maximum velocities are 1.66 m/s and 1.30 m/s for c and d, respectively.

The only exception is the northward flow along the upper eastern wall in the southern part of the channel (Fig. 6c). The north–south section (Fig. 7) shows that the overflow is much more vigorous in the forced than in the density-driven case and, consequently, the cyclonic eddy is enhanced. The eddy formation in the southern basin begins near the bottom by rotation of the dense fluid. It has been described as dome-shaped by Gill (1977) and, in relation to a convective chimney, by Killworth (1992). In our case, both density gradient and topography are important for the formation of this dome. The existence of such an eddy is well established under stationary conditions. However, additional numerical experiments show that the number of eddies and their salinity depend on the preconditioning of the flow. A spin-down experiment was done (not shown), in which the barotropic forcing was switched off after 4 days. Immediately two small eddies were generated near the main eddy, one of them was anticyclonic. All eddies propagated away from the sill. Thus, under unstationary conditions the situation becomes more complicated.

The energy cycle (Fig. 8) shows the external kinetic energy being dominant and amounting to 74.2% of the total kinetic energy. The terms in Fig. 8 have the same meaning as described in the density-driven case. Both kinetic and potential energy have increased relatively to the previous

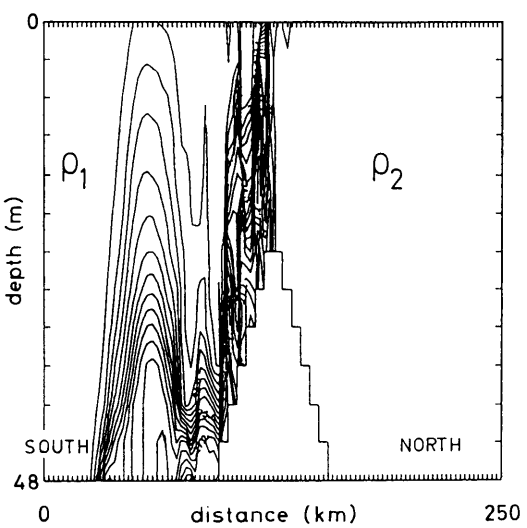

Fig. 7. Density field along the channel in the forced case. Location of the section is given in Fig. 2.

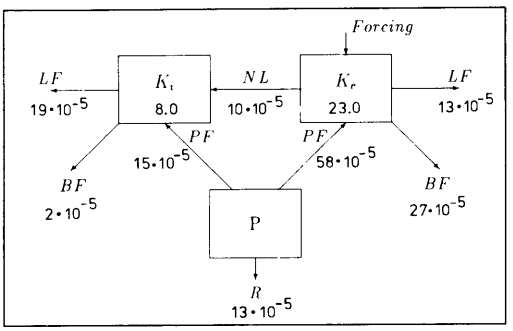

Fig. 8. Energy cycle for the forced case. Energy transfers are shown by arrows in J m^{-3} s^{-1}.

experiment. Most of the initial kinetic energy is used for the rapid eddy formation within approximately one inertial period. Velocities have increased especially in the lower layer, where the barotropic mode and the first baroclinic mode of the density driven current are in phase. Mixing is stronger in comparison to the density-driven case (term R in Fig. 8). The pressure force that transfers energy from potential to external kinetic energy, increased by a factor 100. The direction of the energy transfer between internal kinetic energy and external energy is opposite compared to the density-driven case.

Whereas the net volume transport is almost zero in the density-driven case, it increases to $28 \cdot 10^4$ m^3 s^{-1} in the forced one. Thus, net inflow into a basin depends mainly on the barotropic sea level inclination.

3. The Baltic experiment

The model is now applied to a more realistic approximation of the Danish Straits. As in Fig. 1, the area extends from the Kattegat towards Bornholm (Fig. 9). Our objective is to check whether the transport ratios between Belt and Sound, mainly deduced from light vessel observations, are consistent with the model transports in the forced case. The grid distance of 2.5 km has been maintained but the vertical resolution is now 5 m (12 layers). Initial distributions for salinity and temperature in the Arkona basin and in the Kattegat are taken from Bock (1971) and Lenz (1971), representing climatological values. The transition between the Kattegat water and the

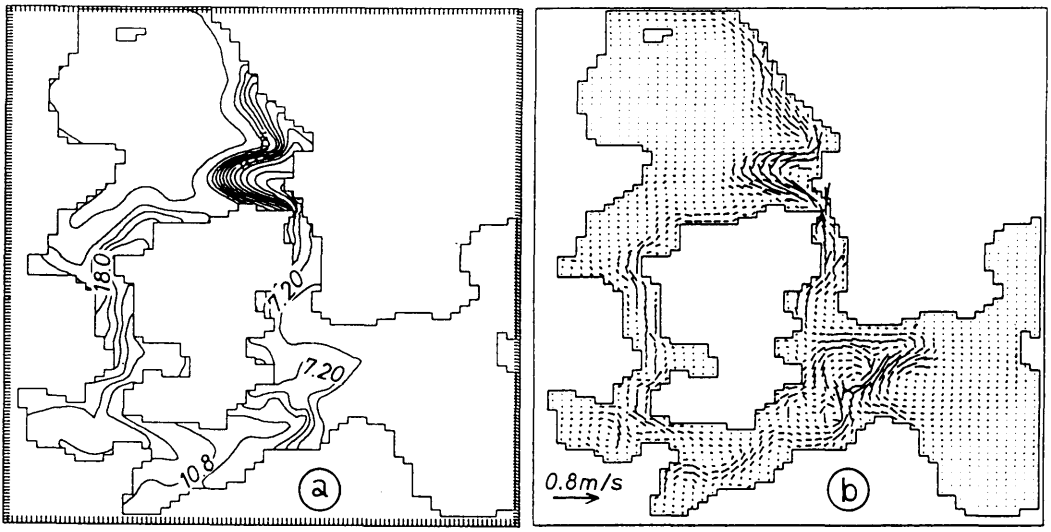

Fig. 9. Thermohaline driven circulation in the Danish Straits after 12 days. (a) Surface density σ_T, (b) surface velocities (layer 1). Maximum velocity is 0.61 m/s, contour increment in (a) is $\Delta\sigma_T = 0.9$.

Baltic water in the straits is assumed to be continuous in T and S between the ends of the straits. Results are presented after 12 days of model run.

Barotropic forcing is simulated by maintaining the sea level in narrow strips of 10–15 grid points near the northern and eastern boundaries. The initial values change linearly over the area. Typically, $\Delta\eta = 0.2$ m or $\Delta\eta = 0.4$ m are used. An additional case with westerly winds is also described.

Compared to the two-basin experiment, the topography is smoother in reality, but the coast lines become more complicated.

3.1. Density-driven flow

Model results for the purely density-driven case are depicted in Fig. 9. After 12 days, Baltic water has penetrated into the Kattegat with a strong baroclinic component. On the other hand, the flow in the Arkona Basin is more or less barotropic. Note the eddies that are formed in the western Arkona Basin. They have much in common with the dome in Fig. 4.

The flow in the Belts and in the Sound is shown in Fig. 10. Inflow into the Baltic occurs in the Great Belt in the deepest part of the cross section with maximum speed of 0.24 m/s (Fig. 10b). Maximum outflow is located at the same position. Contrary to that, in the Fehmarnbelt inflow into the Baltic is observed in the entire water column of the left half of the channel and outflow occurs at the eastern side. This implies that part of the saline water of the deeper layers is transported back towards the north. In the Belt strong mixing is observed, as evident from the change in salinity (Fig. 10a, c).

In contrast to the Belt with its typical bi-directional current system, outflow into the Kattegat extends over the entire Sound, reaching maximum velocities of 0.20 m/s near the surface.

The time history of the transport through Belt and Sound is shown in Fig. 11. When the model starts, inflow into the Baltic occurs in both straits due to the density gradient. After 2 days, the circulation system of Fig. 9 is established.

Obviously, this circulation finally comes to rest and light Baltic water overlays the heavier water of the Kattegat in the entire domain. However, the 12-day range shown in Figs. 9–11 is of interest during calm periods without sea level differences, which seldom exceed one week. Note that net inflow through the Belt and outflow through the Sound balance each other after about 3 days, which is to be expected in cases with river runoff being neglected.

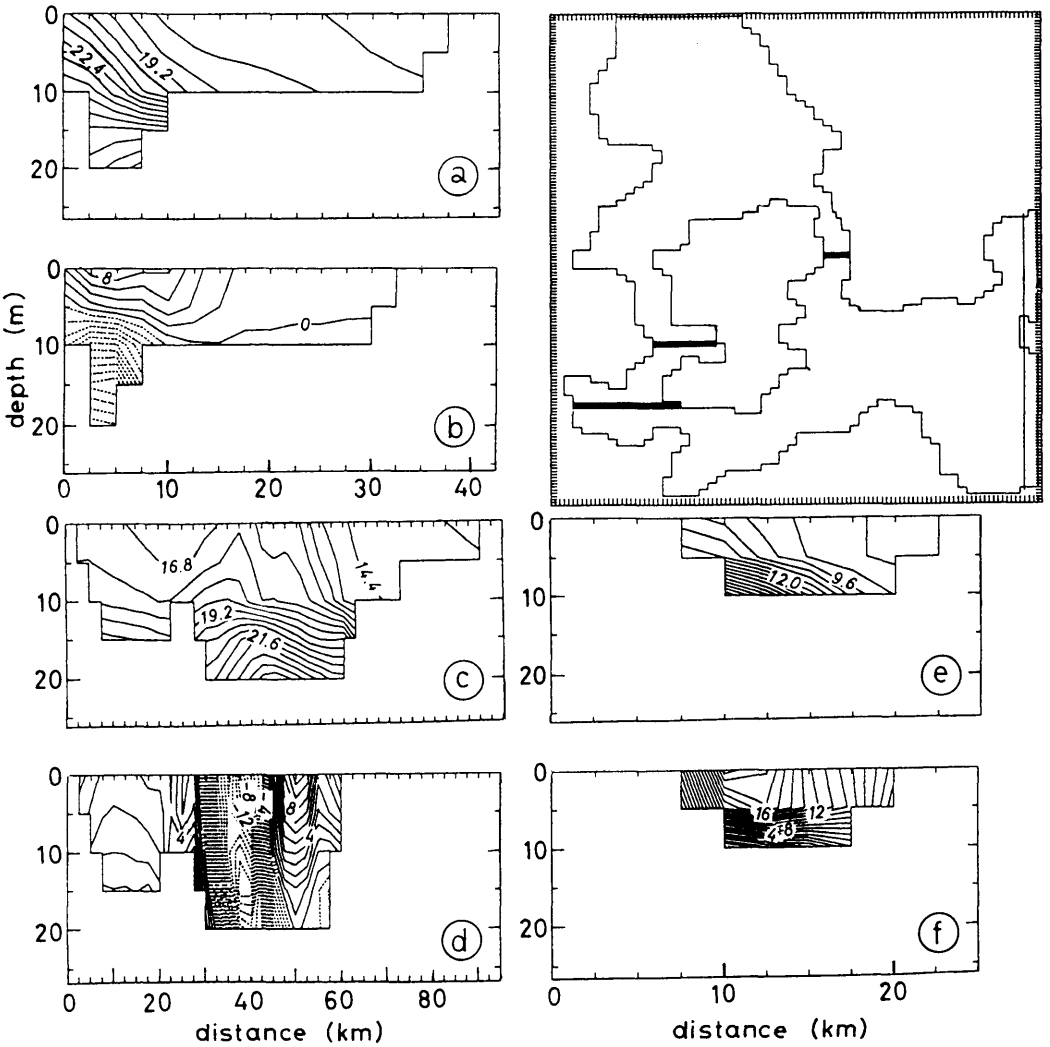

Fig. 10. Salinity (a) and currents (b) in the Great Belt, the Fehmarn Belt (c) and (d), and in the Sound (e) and (f). Location of sections is shown in the upper right panel (velocities in 10^{-2} m/s). Bottom topography appears different for S and v due to the numerical grid for S and v.

3.2. Barotropic forcing

Imposing a sea level difference of $\Delta\eta = 0.20$ m between Bornholm and the northern Kattegat we produce in- and outflow circulation patterns, depending on the sign of $\Delta\eta$. These are shown in Figs. 12 and 13. During inflow the sea level is lower in the Arkona Basin than in the Kattegat. The inflowing dense water (Fig. 12a) is separated from the water in the neighbouring bays by a marked front at the surface. The water penetrates until Darss Sill. In the Sound the front between the two water masses is shifted towards the southern entrance. The inflowing water through Sound and Belt merge in the western Arkona Basin. Also in the barotropic case we observe the formation of a cyclonic eddy east of Darss Sill and an associated anticyclonic one further to the northeast. During

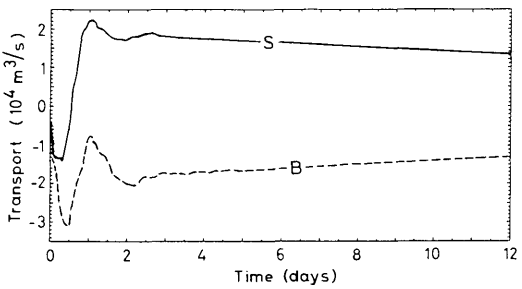

Fig. 11. Transport through Belt (*B*) and Sound (*S*). Units in 10^4 m^3/s.

outflow (Fig. 13), when the sea level in the Arkona Basin is higher than in the Kattegat, strong currents are observed in the Sound, yielding a marked front parallel to the Swedish coast (Fig. 13a, b). Comparison of the surface currents with the barotropic currents (not shown) reveals that the flow is mainly barotropic. This becomes more evident by considering the cross sections (Fig. 14).

The direction of the currents is different from the thermohaline case. Generally, in the entire water column the velocities are to the south in case of inflow and to the north in the outflow case. Only in the Belts, and in the outflow case, the barotropic forcing used is not strong enough to overcome the thermohaline component in the bottom layer completely.

Maximum velocity values for inflow are always larger than for outflow, although the strength of the barotropic forcing is the same in both cases. The reason for this seems to be that during outflow continuous stratification is maintained ("no topographic breakthrough", Killworth, 1989), and coastal trapped waves develop in the outer part of the channels.

After the quasi-steady state is reached in the Great Belt (Fig. 14a, b), maximum velocities are 0.80 m/s for inflow and 0.30 m/s for outflow in the upper layer. In the lower layer corresponding values are 0.24 m/s for inflow and 0.12 m/s for outflow. In the Sound (Fig. 14c, d) maximum velocities during inflow reach 0.36 m/s and 0.27 m/s in the upper and lower layers, respectively, and 0.20 m/s and 0.16 m/s during outflow. Maximum velocities during outflow occur in the upper layer both in the Belts and in the Sound. In case of inflow, barotropic and baroclinic components partially cancel each other in the upper layer. Consequently, maximum velocities must occur in the lower layer, where the thermohaline and the barotropic currents flow into the same direction. This can also be explained by the

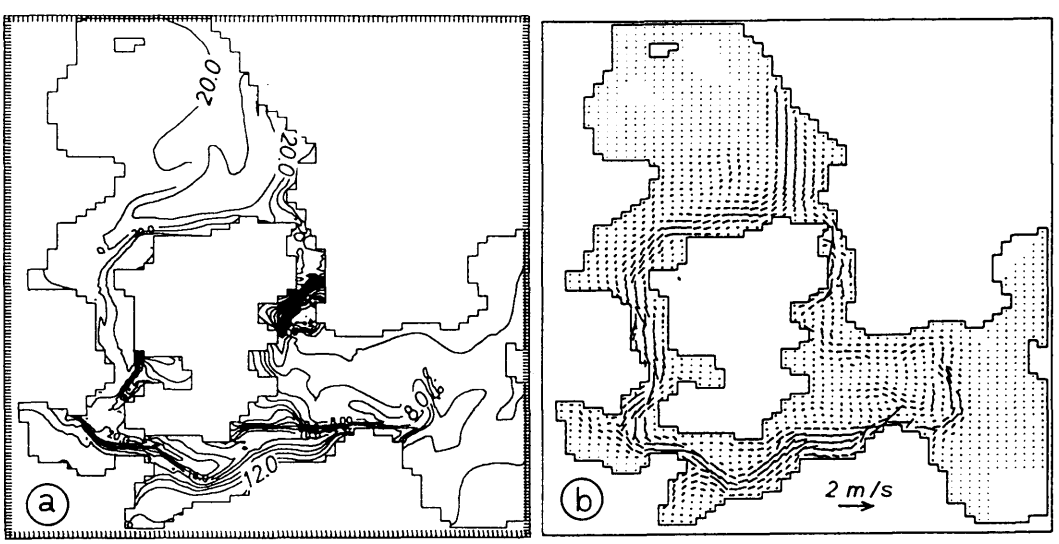

Fig. 12. Inflow circulation pattern after 12 days. (a) Surface density (σ_T), (b) surface velocities (layer 1). Maximum velocity is 1.83 m/s.

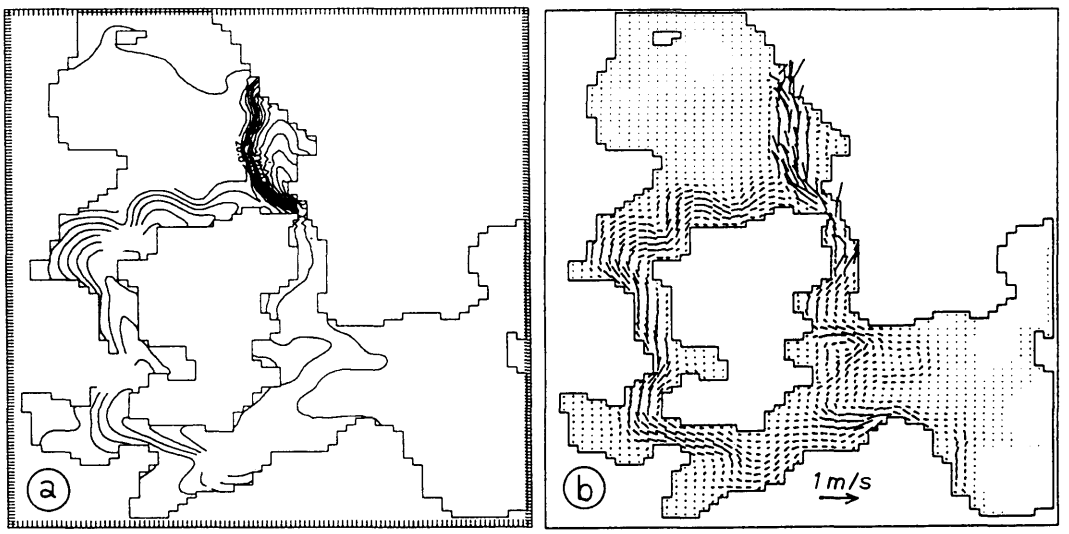

Fig. 13. Same as Fig. 12 for the outflow case. Maximum velocity is 0.81 m/s.

hydraulic theory (Stigebrandt, 1980; Baines and Granek, 1990). According to this theory, a significant amount of water flows in the lower layer if the Froude number $F > 1$. In the present study it is found that the Froude number is always greater than 1 for the inflow case. During almost all of the time the maximum velocity values in the upper layer of the Sound are smaller than the values in the Belt for both inflow and outflow (compare Fig. 14a, b and 14c, d). On the other hand, in the lower layer maximum velocity values in the Sound are larger than the values in the Belt for both inflow and outflow. An additional experiment was performed to determine the effect of wind forcing. The wind stress is chosen to be constant in x-direction ($\tau = 0.2$ kg m^{-1} s^{-2}), and the same sea level difference between the northern and eastern boundary is used as in the previous experiments.

Due to local winds, the results are modified by an Ekman layer. Velocities decrease gradually from the surface to the Ekman depth. Compared to the case without wind forcing, maximum velocities are found in the upper layer in the middle of the channel and not in the lower layer. Vertical homogenization of the upper layers is well pronounced in the salinity field. Also the horizontal salinity differences are smaller across the straits.

We finally note a change in the speed of the propagating salinity front. At the beginning of the adjustment process, and without wind, the salt front propagates with 26.8 km/day; this value reduces to 16.0 km/day at the end of day 12. In the wind driven case the front proceeds slightly faster during the first adjustment phase (28.5 km/day), declining to 15.9 km/day at day 12. The calculated speeds at the beginning of the adjustment are in both cases close to the values observed for mid-November 1976 by Lass and Schwabe (1990). They found 0.30 m/s (25.9 km/day). Contrary to the inflow case, the propagation of the front in the outflow case is very slow, approximately 2.8 km/day.

The model produces a much stronger inflow than outflow in the upper layers under equal but opposite external forcing. This in good agreement with observations. Dietrich (1951) found that during westerly winds of Bft 6 at light vessel Fehmarnbelt inflow occurs at a speed of 1 m/s, whereas during Bft 6 from the east only 0.7 m/s are observed.

The volume transport through the straits is strongly influenced by sea level inclination and wind. Whereas in the density driven case $1.2 \cdot 10^4$ m^3/s left the Arkona Basin through the Sound, and the same amount entered the basin as

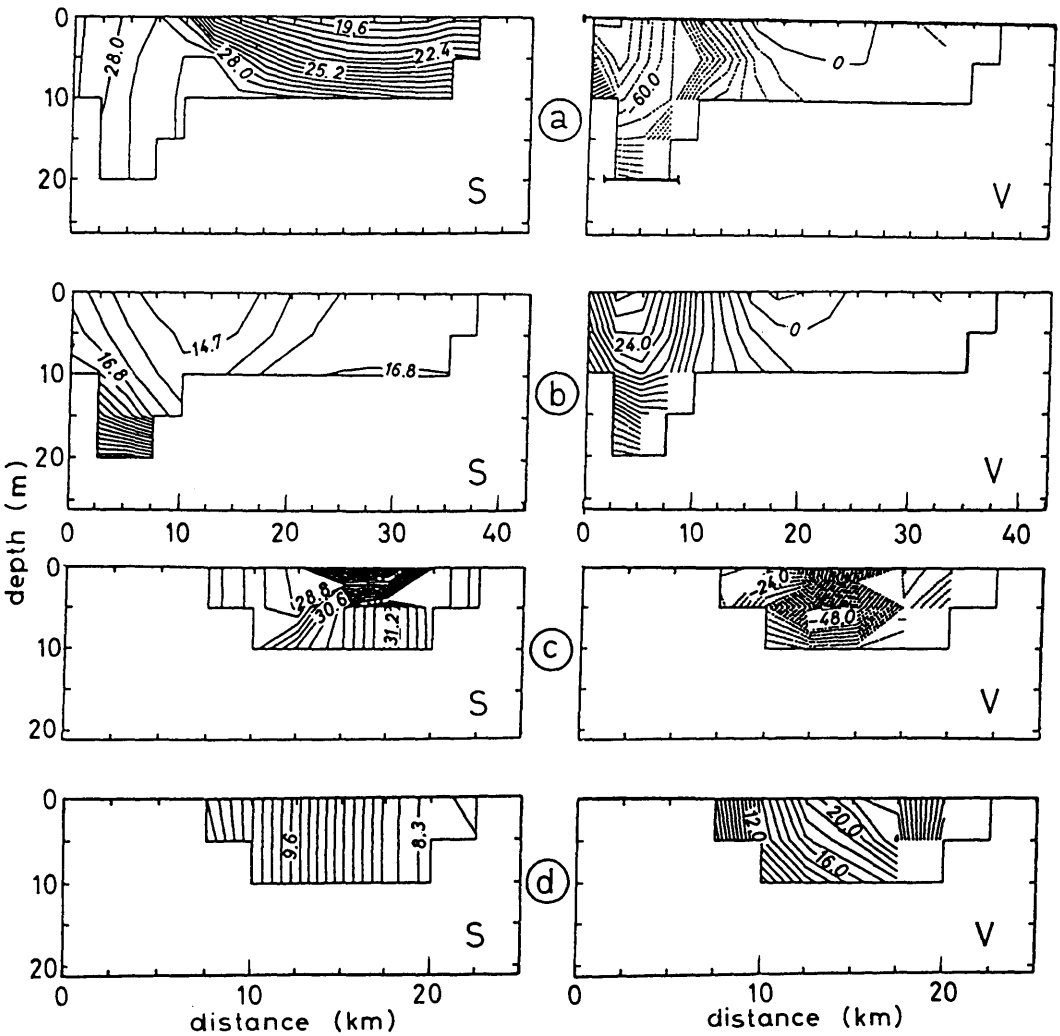

Fig. 14. Salinity and current distributions (currents in 10^{-2} m/s). (a) Inflow and (b) outflow in the Great Belt. (c) Inflow and (d) outflow in the Sound.

net transport through the Belt, volume transport increases by an order of magnitude due to sea level inclination. The values are listed in Tables 1 and 2 for initially strong and weak transitions from Baltic water to Kattegat water in the straits, respectively. In case of weak transition, we assumed a linear transition in T and S between Bornholm and the northern Kattegat, instead of having this entire gradient located within the straits. For weak transition, a general ratio of 71% : 29% can be assumed for the volume transport in Belt and Sound, both for inflow and out-

Table 1. *Volume transport (10^4 m^3/s) through the Danish Straits in case of strong transition*

	Sea level $\Delta\eta = 0.2$ m			$\Delta\eta = 0.4$ m	
	inflow	outflow	inflow with wind	inflow	outflow
Belt	11.9 75.0%	3.15 59.0%	14.4 72.0%	16.7 73.6%	10.0 69.5%
Sound	4.0 25.0%	2.2 41.0%	5.6 28.0%	6.0 26.4%	4.4 30.5%

Table 2. *Volume transport (10^4 m^3/s) through the Danish Straits in case of weak transition*

	Sea level $\Delta\eta = 0.2$ m		$\Delta\eta = 0.4$ m	
	inflow	outflow	inflow	outflow
belt	10.7	5.4	15.1	11.2
	72.3%	70.1%	71.6%	70.9%
sound	4.1	2.3	6.0	4.6
	27.7%	29.9%	28.4%	29.1%

flow (Table 2). If the initial transition occurs within the straits (Table 1) the ratio is still similar except for weak sea level inclination (0.2 m) in the outflow case. During outflow, $\Delta\eta = 0.2$ m is obviously not strong enough to overcome the pressure gradient associated with the density difference along the Belt in the deeper layers, resulting in a much weaker outflow.

4. Relation between surface elevation and volume transport

The confinement of the flow by a strait can give rise to profound dynamical consequences including hydraulic control. As outlined in the introduction the concepts of hydraulics have recently been applied also to large-scale geophysical flows. However, these flows can be strongly influenced by the earth's rotation when the Rossby radius of deformation is the same order of or smaller than the width of the strait. Geostrophy may eventually dominate the flow (geostrophic control). In this section we investigate the validity of the appropriate relations. Pratt (1991) compared the hydraulic flow with geostrophic flow and gave some initial conditions and a number of restrictions for both controls. According to that, geostrophic control breaks down when the Kelvin waves and the associated boundary current have passed the channel. The second limitation is that the system must be restricted to small amplitude motions. This means that the difference between the surface elevations in the two basins or the isopycnal levels must be smaller than the depth of the channel by an order of magnitude.

The volume transport through the Belt has been discussed by a number of authors. Svansson (1980) and Stigebrandt (1980) applied the Helmholtz resonator principle, Welander (1974), Stigebrandt (1983) and Farmer and Møller (1990) tried to describe the exchange of water in the Belt by means of the hydraulic relation. The geostrophic water exchange was studied by Toulany and Garrett (1984), Lass and Schwabe (1990) and Lundberg and Walin (1990). Another approach (not related to the Belt) is that by Whitehead (1986), who added a second term to the hydraulic relation, arising from lateral shear due to rotation. Except for the Helmholtz resonator, these relations will be compared with our model results. The expressions for the transport are as follows:

geostrophic relation

$$Q_g = gh\,\Delta\eta/f, \tag{1}$$

hydraulic relation

$$Q_h = Wh(2g\,\Delta\eta)^{1/2}, \tag{2}$$

Whitehead's hydraulic equation

$$Q_w = Q_h - 1/2 f W^2 h. \tag{3}$$

Here, g is the acceleration of gravity, f is the Coriolis parameter, W is the width of the strait, h is the depth, and $\Delta\eta$ is the difference in surface elevation across the channel. The hydraulic relation is based on surface elevations along the channel, but cross channel elevations can be used in the hydraulic relation if the assumption made by Toulany and Garritt is valid. This assumption requires that the difference in sea level along the strait is equal to the difference across the strait. Following Lass and Schwabe (1990), the longitudinal sea level difference between the Baltic and the Kattegat forces a transverse one. They obtained a correlation coefficient of 0.65 for this assumption. They also found that the transverse gradient adjusts within one inertial period. However, the transverse gradients amounts only to about half of the longitudinal one.

Internal hydraulic control is not included in the test; it is unlikely that this is important. Farmer and Møller (1990) analysed for the Great Belt that only for about 15% of the available time series the flow was hydraulically controlled. But even then it arose from strong barotropic forcing.

To obtain the transport as function of $\Delta\eta$ we changed the longitudinal sea level difference

linearly with time, resulting in corresponding transverse gradients. In Fig. 15 we depict the relations (1) to (3) together with the model transport as function of transverse sea level difference for inflow and outflow, respectively. These show that the geostrophic relation holds in the Sound both for inflow and outflow (Fig. 15b, d). However, a systematic shift of about $1 \cdot 10^4$ m^3/s is observed.

The geostrophic relation does also hold for outflow in the Belt, but the shift is even $3 \cdot 10^4$ m^3/s.

These shifts are due to the baroclinic contribution to the mass transport. As seen from the salinity sections in Fig. 14, even for unidirectional flow stratification is maintained. Consequently the mass transport includes two components, the barotropic and the baroclinic one. This is also

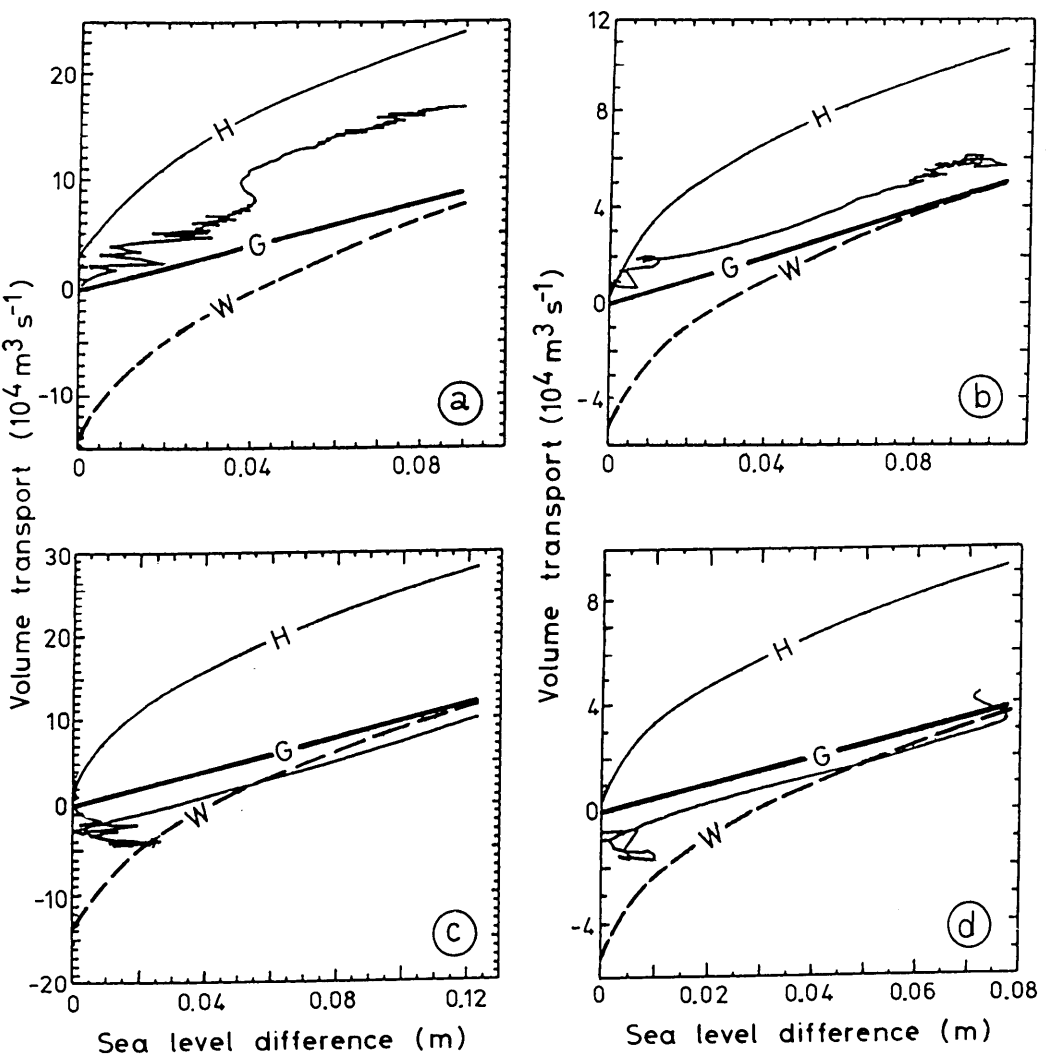

Fig. 15. Comparison of the relations (1)–(3) (H = hydraulic, G = geostrophic, W = Whitehead's hydraulic relation) with the calculated volume transport of the model (full line without symbol). Volume transport is shown as function of sea level difference across the straits. (a) inflow in the Belt (b) inflow in the Sound (c) outflow in the Belt (d) outflow in the Sound. Note the different scales for Belt and Sound.

evident from Figs. 12a, b and 13a, b. For a rectangular cross section F the geostrophic mass transport is given by

$$V = \frac{gF}{f}\frac{\partial \eta}{\partial x} + \frac{g}{f\rho_0}\int_{-H}^{0}\left\{\int_{z}^{0}\left[\rho(x_E, z) - \rho(x_W, z)\right] dz'\right\} dz, \quad (4)$$

where $\rho(x_E, z)$ and $\rho(x_W, z)$ are the vertical density distributions at the eastern and western bank of the cross section, respectively, and η is supposed to vary linearly with x. For outflow, the fresher water is on the eastern side (see Fig. 14b, d) and thus the second term in (4) is negative, yielding the negative shift of the curves in Fig. 15c and d. For inflow this term is positive and consequently the shift is in opposite direction. The larger shift in the Belt results from the stronger density difference compared to the Sound.

The more complicated curve for inflow through the Belt (Fig. 15a) can be approximated by two segments according to the geostrophic relation, with a jump near $\Delta\eta = 0.04$ m. This jump results from inflow of denser Kattegat water. With $\Delta\eta = 0.04$ m the associated barotropic current exceeds 0.10 m/s. Then the outflow at the eastern side of the Belt collapses and the current becomes unidirectional. A strong salinity gradient results between the saline inflowing water on the eastern side of the Belt and the fresher water in western bays, adding a strong baroclinic component to the mass transport.

We conclude that the geostrophic relation holds both for inflow and outflow in the Belts and in the Sound, but different baroclinic transports have to be added to the barotropic relation. The geostrophic control is not surprising; it could be expected from Figs. 12 and 13, which show that both the dominant sea level gradients (not depicted) and the density gradients are in cross direction in the straits, except for inflow in the northern part of the Sound. South of Helsingör-Helsingborg obviously more water is discharged than can be replaced through this narrow in the Sound. The hydraulic control relation is neither supported for the Belts nor for the Sound by the model results.

The validity of the geostrophic relation for the flow through the Belt is in good agreement with observations. Measurements of currents, stratification and sea level across the Fehmarnbelt during 1936 (Jacobsen, 1980) gave the following relation for the transport: $V(\mathrm{m^3/s}) = 12.8\,\Delta\eta\,(\mathrm{m})$, where $\Delta\eta$ is the sea level difference between Rödbyhavn and Marienleuchte. The correlation coefficient was 0.96. Jensen and Sinding (1945) compared the geostrophic relation between Slipshavn and Korsør in the Great Belt to surface currents at Halskov Rev lightship in the period 1923–1929 and found good correlation for monthly averages. Lange (1974), based on hydrographic and current measurements, also demonstrated that the currents in the Fehmarnbelt are correlated with the transverse sea level difference. Thus, our results are sufficiently supported by observations in the Belts.

Fig. 15 shows that the geostrophic relation is also fulfilled in the Sound. This is only an apparent contradiction to barotropic models that have been used to simulate the transport through the Sound (Jacobsen, 1980). They are based on $g\,\partial\eta/\partial y = -\tau_B^{(y)}/\rho H$, where η is sea level, $\tau_B^{(y)}$ bottom stress (assumed to be proportional to the square of the transport Q) and H is water depth. This yields a relation $Q = K\,\Delta\eta/|\Delta\eta|^{1/2}$ (square-root model of Jacobsen), where K is empirically determined as $K = 9 \cdot 10^4\ \mathrm{m^{5/2}\,s^{-1}}$. According to this, the meridional sea level inclination should be balanced by the bottom stress. However, this implies that the Coriolis force is balanced by the zonal difference in sea level and the wind stress, $g\,\partial\eta/\partial x = fv + \tau_0^{(x)}/\rho H$. For vanishing wind stress, this is exactly our geostrophic relationship.

That the geostrophic relation holds in the southern Sound becomes also evident by comparing surface currents at Drogden with the sea level gradients Copenhagen-Klagshamn, which are generally used in the square-root model. The line which connects Copenhagen tide gauge with Klagshamn is oriented NW–SE (and not N–S, see Fig. 1). The currents at Drogden light vessel are known to have nearly always either the direction NE (outflow) or SW (inflow), as shown by Dietrich (1951). Thus the sea level gradient Copenhagen-Klagshamn is oriented perpendicular to the current, just describing the geostrophic flow. Figs. 12 and 13 show, for inflow and outflow conditions, that also our numerical model yields these two flow directions near Drogden. Instead of using the balance between bottom stress (with unknown friction coefficient) and sea level inclination in

along-current direction (which is not available) it would be much more logical to use directly the geostrophic relation.

From the shift of the thin curves in Fig. 15 relative to the barotropic curve G we conclude that an increase of the cross-strait sea level difference $\Delta\eta$ by 0.01 m increases the mass transport by $0.5 \cdot 10^4$ m^3/s and $1 \cdot 10^4$ m^3/s in Sound and Belt, respectively. To obtain the same values by the along-strait density difference, $\Delta\sigma_T$ would have to be raised by $\Delta\sigma_T = 6$ kg/m^3 in the Sound and $\Delta\sigma_T = 4$ kg/m^3 in the Belt, except for strong inflow. Under inflow conditions with $\Delta\eta > 0.04$ m across the Belt, mass transport increase by $1 \cdot 10^4$ m^3/s already for $\Delta\sigma_T = 1.3$ kg/m^3. This shows that inflows of saline water into the Baltic are strongly enforced by heavy water in the southern Kattegat, being the only real possibility to enlarge the density difference. Thus, raising water with high salinities from the deeper layers of the southern Kattegat is an important precondition for major inflow events.

By using the relations depicted in Fig. 15, one has to bear in mind that they are derived from quasi-steady conditions, i.e., without local wind influence and without varying baroclinic conditions. In actual data, under time-variable conditions, the baroclinic contribution in (4) may yield a large scatter. This is supported by additional numerical model results (not shown). We computed the transports through Belt and Sound, each for a 12-day period in January, July, September and November 1989, using the actual wind over the area and the observed sea level data from the tide gauges within the restoring zones in the Kattegat and in the Arkona Basin. This shows that the actual transport ratio between Belt and Sound cannot be deduced using a fixed relation. We conclude that only under quasi-steady conditions the barotropic geostrophic relation with baroclinic correction is a good approximation to the real transport.

5. Conclusions

Within Baltex, an international regional program of the global energy and water cycle experiment (GEWEX), a hierarchy of models is used at IfM Kiel, including a high resolution model of the western Baltic with active open boundaries, using the method described by Stevens (1990). For the present case study that concentrates on the flow in the Danish Straits due to artificially prescribed sea level and density differences between the Kattegat and the central Baltic, a simple approach with restoring zones is justified. Comparisons with the Baltex models show that in both cases the structure of the current field in the Danish Straits is essentially the same.

The model results show that the flow through the Danish Straits is largely enhanced by sea level differences between the Kattegat and the Baltic. In the density-driven case, the water exchange gains its energy from the available potential energy, given by the density difference between the water masses of the Kattegat and the Baltic. The flow is bi-directional in the Belt and relatively weak. Outflow occurs in the Sound. The inflowing water in the Belt forms eddies in the western Arkona basin which have much in common with the dome-like structure under ideal conditions. These eddies prevent the heavy water from passing rapidly through the Arkona Basin. The process is important for the renewal of deep water in the Bornholm and Gotland basins. The longer the heavy water in the Arkona basin is exposed to wind stirring, the more becomes its salinity reduced by mixing with upper layer water. Thus, the inflowing water cannot replace the heavier bottom water in the deeper basins.

Sea level inclination changes the energy cycle considerably, resulting in strong barotropic currents. Both in the Belt and in the Sound the flow is geostrophically controlled. However, due to the baroclinic field the transport cannot be computed from the sea level inclination without correction.

It is generally assumed that the transport ratio between Belt and Sound is 70 % : 30 %. The model results show that this can be confirmed under steady conditions and dominance of the barotropic flow. However, if the sea level difference between Arkona basin and Kattegat becomes small and the transition zone between Baltic and Kattegat water is confined to the Belt Sea, the baroclinic flow becomes very important in the Belt and reduces the ratio to 59 % : 41 % (Table 1). As the transition zone seldom passes the borders of the Belt Sea care should be taken by applying any fixed relation in the outflow case. Under variable wind conditions no fixed ratio can establish.

Therefore, a detailed analysis of the mass and salt transport through the Danish Straits can only be obtained by a high-resolution numerical model.

The present paper concentrates on a few case studies of processes which play an important rôle in the water exchange between Kattegat and Baltic.

(i) The formation of a dome-like cyclonic eddy in the Arkona basin by the inflowing salty water from the Kattegat

(ii) The influence of the baroclinic field on the ratio of mass transports through Belt and Sound and

(iii) The possibility of hydraulic control in the straits.

Using restoring zones for the description of sea level differences between Kattegat and Baltic considerably reduces the numerical expenses. A similar approach is used for ocean models by prescribing temperature and salinity within restoring zones near arbitrarily closed boundaries. In our case the sea level within the restoring zones results from the large-scale wind effects on the sea level outside the model domain, much the same as temperature and salinity within the restoring zones of ocean models result from water mass formation outside the domain of these models.

The application of such a limited area model is only possible for short time scales, until the baroclinic field is advected towards the restoring zones. To describe in- and outflow through the Danish Straits over longer periods and for real forcing, open boundary conditions have to be used. The combination of a hierarchy of models with data assimilation holds promise for greatly enhancing our understanding of the highly variable transports trough the Danish Straits.

REFERENCES

Baines, P. G. and Granek, H. 1990. Hydraulic models of deep stratified flows over topography. In: *The physical oceanography of sea straits*, ed. L. J. Pratt. Kluwer, Boston, pp. 245–269.

Bock, K. H. 1971. Monatskarten des Salzgehaltes der Ostsee. *Ergänzungsheft zur Deutschen Hydrographischen Zeitschrift*, Reihe B, nr. 12.

Bormans, M. and Garrett, C. 1989. The effect of rotation on the surface inflow through the Strait of Gibraltar. *J. Phys. Oceanogr.* **19**, 1535–1542.

Böning, C. W. 1989. Influences of a rough bottom topography on flow kinematics in an eddy-resolving circulation model. *J. Phys. Oceanogr.* **19**, 77–97.

Bryden, H. L. and Kinder, T. H. 1991. Steady two-layer exchange through the Straits of Gibraltar. *Deep-Sea Res.* **38**, 445–463.

Dalziel, S. B. 1990. Rotating two-layer sill flows. In: *The physical oceanography of sea straits*, ed. L. J. Pratt. Kluwer, Boston, pp. 343–371.

Dietrich, G. 1951. Oberflächenströmung im Kattegat, im Sund und in der Beltsee. *Dt. Hydrogr. Z.* **4**, 129–150.

Farmer, D. M. and Møller, J. S. 1990. Measurements and modeling in the Great Belt. A unique opportunity for model varification. In: *The physical oceanography of sea straits*, ed. L. J. Pratt. Kluwer, Boston, pp. 125–152.

Garrett, C., Bormans, M. and Thompson, K. 1990. Is the exchange through the Strait of Gibraltar maximal or submaximal? In: *The physical oceanography of sea straits*, ed. L. J. Pratt. Kluwer, Boston, pp. 271–294.

Gill, A. E. 1977. The hydraulics of rotating-channel flow. *J. Fluid Mech.* **80**, 641–671.

Hogg, N. G. 1983. Hydraulic control and flow separation in a multi-layered fluid with applications to the Vema Channel. *J. Phys. Oceanogr.* **13**, 695–708.

Hogg, N. G. 1985. Multilayer hydraulic control with application to the Alboran sea circulation. *J. Phys. Oceanogr.* **15**, 454–466.

Jacobsen, J. P. 1925. Die Wasserumsetzung durch den Öresund, den Großen und den Kleinen Belt. *Medd. Komm. Havundersögelser, Ser. Hydr. Copenhagen* **2**:9, 71 pp.

Jacobsen, T. S. 1980. *Sea water exchange of the Baltic. Measurements and methods.* The National Agency of Environment Protection Denmark, 106 pp.

Jensen, H. and Sinding, E. 1945. On the difference between the heights of the mean sea level at the self-recording tide-gauges at Korsör and Slipshavn. *Geodaetisk Institut, Medd.* nr. 20.

Killworth, P. D. 1989. Transmission of a two-layer coastal Kelvin wave over a ridge. *J. Phys. Oceanogr.* **19**, 1131–1148.

Killworth, P. D., Stainforth, D., Webb, D. J. and Paterson, S. M. 1989. A free-surface Bryan-Cox-Semtner model. *Inst. of Oceanogr. Sciences Deacon Laboratory Report*, no. 270, 184 pp.

Killworth, P. D. 1992. The time-dependent collapse of a rotating fluid cylinder. *J. Phys. Oceanogr.* **22**, 390–397.

Lange, W. 1974. *Zu den Ursachen langperiodischer Strömungsänderungen im Fehmarn Belt.* Diplomarbeit, Kiel, 66 pp.

Lass, H. U. and Schwabe, R. 1990. An analysis of the salt water inflow into the Baltic in 1975 to 1976. *Dt. Hydrogr. Z.* **43**, 97–125.

Lehmann, A. 1992. Ein dreidimensionales baroklines wirbelauflösendes Modell der Ostsee. *Ber. Inst. f. Meeresk., Kiel*, nr. 231, 104 pp.

Lehmann, A. 1995. A three-dimensional baroclinic eddy-resolving model of the Baltic Sea. *Tellus* **47A**, in press.

Lenz, W. 1971. Monatskarten der Temperatur der Ostsee. *Ergänzungsheft zur Dt. Hydrogr. Z.*, Reihe B, Nr. 11.

Lundberg, L. and Walin, G. 1990. The distribution of the geostrophic flow in a stratified surface layer. *Tellus* **42A**, 583–593.

Mälkki, P. and Tamsalu, R. 1985. Physical features of the Baltic Sea. *Finn. Mar. Res.*, no. 252, 110 pp.

Omstedt, A. 1990. Modelling the Baltic Sea as thirteen sub-basins with vertical resolution. *Tellus* **42A**, 286–301.

Pratt, L. J. 1991. Geostrophic versus critical control in straits. *J. Phys. Oceanogr.* **21**, 728–732.

Rahm, L. 1985. On the diffusive salt flux of the Baltic proper. *Tellus* **37A**, 87–96.

Stevens, D. P. 1990. On open boundary conditions for three dimensional primitive equation models. *Geophys. Astrophys. Fluid Dyn.* **51**, 103–133.

Stigebrandt, A. 1980. Barotropic and baroclinic response of a semi-enclosed basinto barotropic forcing from the sea. In: *Fjord oceanography*, ed. H. J. Freeland, D. M. Farmer and C. D. Levings, Plenum, pp. 141–163, 715.

Stigebrandt, A. 1983. A model for the exchange of water and salt between the Baltic and the Skagerrak. *J. Phys. Oceanogr.* **13**, 411–427.

Svansson, A. 1980. Exchange of water and salt in the Baltic and adjacent seas. *Oceanologica Acta* **3**, 431–440.

Toulany, B. and Garrett, C. 1984. Geostrophic control of fluctuating barotropic flow through straits. *J. Phys. Oceanogr.* **14**, 649–655.

Walin, G. 1977. A theoretical framework for the description of estuaries. *Tellus* **29**, 128–136.

Welander, P. 1974. Two-layer exchange in an estuary basin, with special reference to the Baltic Sea. *J. Phys. Oceanogr.* **4**, 542–556.

Whitehead, J. A. 1986. Flow of a homogeneous rotating fluid through straits. *Geophys. Astrophys. Fluid Dyn.* **36**, 187–205.

Wyrtki, K. 1954. Die Dynamik der Wasserbewegungen im Fehmarn Belt II. *Kieler Meeresf.* **X**, 162–181.